Clay Minerals, (2015) **50**, 431–440

Grey Oxisol from the Jequitinhonha Valley, Minas Gerais, Brazil: a conceptual challenge to the soil classification system?

A. C. SILVA[1], E. MURAD[1,*], J. D. FABRIS[1], S. DE SOUZA[1], M. J. MENDES PIRES[1], M. C. PEREIRA[2], A. O. GUIMARÃES[3], H. VARGAS[3] AND J. D. ARDISSON[4]

[1] *Universidade Federal dos Vales do Jequitinhonha e Mucuri (UFVJM), 39100-000 Diamantina, Minas Gerais, Brazil*
[2] *Instituto de Ciência, Engenharia e Tecnologia, Universidade Federal dos Vales do Jequitinhonha e Mucuri (UFVJM), 39803-371 Teófilo Otoni, Minas Gerais, Brazil*
[3] *Universidade Estadual do Norte Fluminense (UENF), 28013-600 Campos dos Goytacazes, Rio de Janeiro, Brazil*
[4] *Centro de Desenvolvimento da Tecnologia Nuclear (CDTN), 31270-901 Belo Horizonte, Minas Gerais, Brazil*

(*Received 4 April 2015; revised 27 June 2015; Associate Editor: Balwant Singh*)

ABSTRACT: The upper Jequitinhonha Valley is located within the Serra do Espinhaço Meridional mountain range in the State of Minas Gerais, Brazil. The topography is flat or gently undulating with large flat areas known as *chapadas* ('high plains') that are dissected by rivers forming swamps known locally as *veredas* ('paths'). The present study is concerned mainly with a representative toposequence in the watershed of the Lagoa do Leandro vereda, a swamp near the city of Minas Novas on a chapada of the highlands of the Alto (Upper) Jequitinhonha region.

The soils of this sequence were studied by a variety of physical and chemical techniques, including Mössbauer, electron spin resonance (ESR) and photoacoustic (PAS) spectroscopies, as well as X-ray diffraction (XRD) and carbon isotope data. Mössbauer spectra of the silt fraction of a grey Xanthic Haplustox (Munsell 10YR 3/2) from the Lagoa do Leandro *vereda*, referred to here as a 'Grey Haplustox' ('LAC'), proved the existence of Fe^{2+}- and Fe^{3+}-bearing components. Photoacoustic spectroscopy confirmed the presence of Fe^{2+}, as shown by Mössbauer spectroscopy, probably in an octahedrally coordinated site, but the principal optical absorption bands are due to different Fe^{3+} sites. A ferrimagnetic contribution and three other paramagnetic lines attributed to Fe^{3+} and Ti^{3+} were demonstrated by means of ESR. The ESR and PAS results are thus in agreement with the chemical composition and Mössbauer spectroscopy, allowing a detailed characterization of the mineralogy of this silt.

Carbon isotope data indicate the climate to have varied during the past: a wetter climate in the Pleistocene, with drier phases in the Late Pleistocene and Holocene, and again a more humid climate 1200 years ago. $\delta^{13}C$ data indicate the C_3 scrubland vegetation to have occupied the bottom of the vereda in the past (Bispo & Silva, 2014).

Greyish Oxisols that consist chiefly of phyllosilicate minerals of the kaolinite group (which are usually associated with binary oxides and hydroxides) are of common occurrence in tropical soils resulting from leaching and precipitation. Such Oxisols of greyish appearance and similar mineralogy have been described elsewhere from Brazil and, for example, from India. Such soils are therefore proposed here as a new hierarchical level of the Soil Classification System.

KEYWORDS: Soil minerals, Magnetization, Mössbauer spectroscopy, ESR, PAS, XRD.

The Jequitinhonha River originates near the city of Diamantina in the Serra do Espinhaço mountain range in the State of Minas Gerais, Brazil, and extends to the lowlands of the eastern coast, most of it in a transitional area from both climatological and geological points of view. The Jequitinhonha valley has a humid climate in its headwaters in the Serra do Espinhaço, is sub-humid in the highlands, semi-arid in its central part and humid again near the mouth of the Jequitinhonha River (Ab´Sáber, 2000). Several aspects of the cerrado

* Email: emurad@yahoo.com
DOI: 10.1180/claymin.2015.050.4.02

landscape domain are also present along the valley. The upper Jequitinhonha valley is flat or gently undulating at an altitude averaging ~900 m with large level areas known as *chapadas* (Portuguese: 'high plains') that are dissected by rivers forming swampy herbaceous corridors referred to locally as *veredas* ('paths') that drain the river basin (Ab´Sáber, 2000; Costa-Milanez *et al*., 2014).

The sediment banks along the *veredas* are aged deposits accumulating sediments from several periods as Cenozoic dendritic sediments. Ancient climatic fluctuations are believed to have occurred more in the interplateau depressions that surrounded or penetrated the regional high plains, which should have been more or less stable in the higher areas (Ab´Sáber, 2000). Regarding human activities, the history of use of the natural resources of the region dates back to the colonial period, when environmentally unconcerned mining for products such as gold and precious stones and unsophisticated agriculture were practiced.

The soils in this region still lack comprehensive studies. In some pedological studies, Ker (1998) observed the occurrence of a grey "Pale Oxisol". In the upper Jequitinhonha valley, Resende *et al*. (1980) identified extensive areas that are dominated by a grey Oxisol. Silva *et al*. (2010) mapped 126,000 ha of land of which 26,500 ha were characterized by a "Grey Oxisol". Bispo *et al*. (2011a,b) described soils of the Lagoa do Leandro *vereda* watershed toposequence by physical, chemical, mineralogical, morphological and micromorphological means, finding a grey soil with all the attributes of an Oxisol and referring to it as a "Grey Haplustox". Ferreira *et al*. (2010) characterized a Grey Oxisol on the basis of a highland toposequence in the upper Jequitinhonha valley. Those authors identified the contributions of chemical and biological (burrowing fauna: ants, termites and worms) processes during the genesis, acting over time on palaeo gley soils that were drained by lowering of the local groundwater level. Teófilo & Frota (1982) also noted the occurrence of a "Grey Oxisol" in the State of Ceará, Brazil. Some Oxisols of greyish appearance consist basically of phyllosilicate minerals of the kaolinite group. Phyllosilicate minerals that are commonly associated with binary oxides and hydroxides are typical of tropical soils resulting from leaching and precipitation.

Silicate minerals consist of silicon bound tetrahedrally to oxygen occurring either as isolated tetrahedral 'islands', or arranged in chains, layers, or networks. Phyllosilicates consist of a layered structure in which two-dimensional planar arrangements of sheets of such corner-sharing oxygen tetrahedra with Si^{4+} as central cation are linked to sheets of edge-sharing octahedra in which oxygens and hydroxyls surround Al^{3+}. Depending on the availability of other elements and the mechanisms of formation, Al can be replaced partially or completely by Mg and Fe (Fe^{2+} and/or Fe^{3+}), and Al and even Fe^{3+} can substitute for Si. Phyllosilicates can therefore contain Fe in octahedral and/or tetrahedral coordination. A detailed, up-to-date rendering of the composition of common minerals including the phyllosilicates and substitutions such as those mentioned above has been given by Deer *et al.* (2013). The substitution by Fe is linked to the charge balance of these minerals, which in turn is related to intrinsic properties of the soil, such as its fertility (Stucki & Kostka, 2006). In kaolinite, Fe^{3+} is more common than Fe^{2+}, although kaolinite may contain significant proportions of the latter (Murad & Wagner, 1991) and higher Fe contents, such as those of many soil kaolinites, are associated with increasing structural disorder (Mestdagh *et al*., 1980).

The hypothesis that the LAC presents mineralogical attributes of Oxisols was tested, as its colour does not fall into this order in the Brazilian System of Soil Classification. In the present study some aspects of the different Fe sites in the LAC are discussed, based on optical absorption data obtained indirectly by means of PAS and ESR measurements. Like Mössbauer spectroscopy and X-ray diffraction (XRD), these techniques are local probes, providing information on specific site configurations, and are backed up here by carbon isotope data on whole soil samples from the same locality.

MATERIALS AND METHODS

The Lagoa do Leandro is located in the municipality of Minas Novas, upper Jequitinhonha valley, Minas Gerais State, Brazil. The bordering coordinates are 17° 19′ and 17° 20′ South latitude, and 42° 28′ and 42° 29′ West longitude. Lithologically this region is dominated by a complex Precambrian sequence comprising quartz-biotite schists with interbedded quartzite, conglomerates, phyllites, limestone lenses, amphibolites and greenschists of the Macaúbas Group (Pedrosa Soares *et al*., 1992).

Soil subgroups identified in accordance with Soil Taxonomy (Soil Survey Staff, 1999) in the toposequence of the Lagoa do Leandro *vereda* were red to grey: a Topic Haplustox ('LVA') at the top, a Xanthic Haplustox ('LA') in the middle and a Grey Haplustox (LAC or '*Latossolo Acinzentado*', literally a 'greyish Oxisol' in Portuguese) at the moderately well drained

https://doi.org/10.1180/claymin.2015.050.4.02 Published online by Cambridge University Press

TABLE 1. Physical and chemical properties of the Bw_2 horizon of the Grey Latosol (LAC) modified after Silva *et al*. (2013) with additional data from Bispo *et al*. (2011a).

Parameter	Value
pH (measured in water suspension)	4.6
pH (Measured in 1 mol L^{-1} KCl 1:2.5 soil/ solution ratio)	3.8
Organic matter [g kg^{-1}]	1.0
Dithionite-soluble Fe (Fed) [g kg^{-1}]	1.75
Oxalate-soluble Fe (Feo) [g kg^{-1}]	0.75
CEC at pH 7.0 [$cmol_c$ kg^{-1}]	3.7
Total sand [g kg^{-1}]	450.0
Fine sand (particle diameter 20–50 μm) [g kg^{-1}]	390.0
Silt (20–2 μm) [g kg^{-1}]	190.0
Clay (<2 μm) [g kg^{-1}]	360.0
Munsell colour	10 YR 3/2

footslope, and a Typic Albaquult ('GXbd') in a swamp covered with palm trees at the bottom (Bispo *et al*., 2011a,b). These soils were described morphologically and chemically and characterized physically by Bispo *et al*. (2011a,b) (Table 1).

The present study was concerned mainly with the Xanthic Haplustox, referred to here as the Grey Haplustox (LAC) that occurs at an altitude of 810–870 m and a distance of 700 m from the Lagoa do Leandro microbasin. Soil samples for the carbon isotope measurements were collected from horizons at depths of 0–9 cm and 25–33 cm at the bottom of the *vereda*.

The iron mineralogy of this soil, mottling of the Bw_2 horizon of which is a significant characteristic, was described in detail by Silva *et al*. (2013). Significant deviations from the interpretations of that study are that here we dispense with the concept of halloysite as a major soil constituent, we present a revised fit of the Mössbauer data which leads to more viable parameters (Fig. 3 and Table 2) – an example of the "non-uniqueness" problem when fitting Mössbauer data (Murad & Cashion, 2004), and include reference to a recent study involving carbon isotope data (Bispo & Silva, 2014).

The silt fraction (particle diameter 20–2 μm) of the LAC sample was obtained by particle sedimentation in aqueous suspension and analysed by the pipette method (Embrapa, 1997), ^{57}Fe-Mössbauer spectroscopy, magnetization measurements, XRD, ESR, PAS and ^{13}C isotopic data.

Chemical analyses were carried out as described by Bispo *et al*. (2011a,b) and Silva *et al*. (2013). Analyses include the determination of Si, Al, Fe, Ti and Mn following digestion of the ground sample in 1:1 H_2SO_4 (EMBRAPA, 1997). Additional analyses by X-ray fluorescence, following the method described by Cheburkin and Shotyk (1996), were carried out on sample batches of 5 g. Better crystalline (hydr)oxides of Fe (Fe_d), and associated Al and Mn were extracted by the dithionite-citrate-bicarbonate method (Mehra and Jackson, 1960; EMBRAPA, 1997), whereas the more poorly crystalline ("amorphous") (hydr)oxides of Fe (Fe_o) and associated Al and Mn were extracted using ammonium oxalate at pH 3.0 in the dark (OAA: Schwertmann, 1964; McKeague and Day, 1966).

Mössbauer spectra were collected at room temperature (298 K) and 80 K using a ^{57}Co source in a Rh

TABLE 2. Mössbauer parameters fitted for the spectra of the silt fraction of the 'Grey Latosol' (LAC) at 298 K and at 80 K. δ: isomer shift relative to α-Fe at 298 K; Δ: quadrupole splitting/quadrupole shift; B_{hf}: magnetic hyperfine field; RA: relative sub-spectral area.

T (K)		δ (mm s^{-1})	Δ (mm s^{-1})	B_{hf} (T)	RA (%)
	Fe^{3+}	0.22	1.0		16
298	Fe^{3+}	0.27	0.55		59
	Fe^{2+}	1.3	0.2		8
	Fe^{2+}	0.98	2.2		17
	Maghemite	0.4	0.0	49.6	9
80	Fe^{3+}	0.27	0.77		61
	Fe^{2+}	1.3	0.6		6
	Fe^{2+}	1.13	2.2		24

https://doi.org/10.1180/claymin.2015.050.4.02 Published online by Cambridge University Press

matrix. The calibration standard was α-iron and all isomer shifts are referred to the centroid of this spectrum. Low-temperature measurements were carried out in a liquid nitrogen flow cryostat. Magnetization measurements were made using a vibrating sample magnetometer with a noise base of $<1 \times 10^{-6}$ emu and a time constant of 100 ms. Powder XRD patterns of the LAC soil were collected using Cu*K*α radiation in the range 4–80°2θ with a step size of 0.02°2θ and a dwell time of 5 s on a Rigaku Ultima IV diffractometer equipped with a graphite diffracted-beam monochromator. Mineral identification was effected by comparison of the sample patterns with those of the International Center for Diffraction Data (ICDD)/Joint Committee on Powder Diffraction Standards (JCPDS) and the Inorganic Crystal Structure Database (ICSD).

For ESR, samples prepared as described were measured in a Bruker Elexsys E500 spectrometer operating at room temperature with microwaves of the X-band (9.5 GHz). The PAS measurements were carried out using a conventional MTEC photoacoustic cell. The radiation source was a xenon arc lamp (600 W) modulated by an SR540 mechanical chopper at 17 Hz. The frequency and sample thickness were chosen to fulfil the requirements for obtaining resolved spectra. A model 77 250 monochromator (Oriel Corp.) was used and the data were recorded scanning the wavelength in 1 nm steps from 300 to 750 nm. The photoacoustic signal was measured by an SR830 lock-in amplifier (Stanford Research Corp.) using the voltage-mode detection.

RESULTS AND DISCUSSION

Chemical analysis showed that Al (~168 g kg^{-1} Al_2O_3), followed by Si (~151 g kg^{-1} SiO_2) predominate in the LAC silt. This has been attributed to the presence of silicates and occluded quartz (Bispo *et al*., 2011a). Total Fe, Ti and Mn were detected at values of ~9 g kg^{-1} Fe_2O_3, 2 g kg^{-1} TiO_2 and 42 mg kg^{-1} Mn. The mottled parts have an Fe content that is ~50% greater than that of the Bw_2 horizon, whereas the contents of the other elements (Al, Si, Ti and Mn) do not vary significantly between the horizons (Bispo *et al*., 2011a). Low levels of Fe in the LAC indicate past reduction processes (Breemen & Buurman, 2002; Coelho *et al*., 2001) that are in agreement with the variations of climate indicated by the carbon isotope data. These processes effected the removal or conversely the concentration of Fe compounds in the form of mottles. The colours are grey (Munsell 10YR 3/2), and the Fe_2O_3/TiO_2 ratio, an important parameter to assess the effects of draining Oxisols, indicates hydromorphism. This Fe_2O_3/TiO_2 ratio is furthermore related to the drainage conditions (Alleoni & Camargo, 1994; Oliveira *et al*., 1991), i.e. the greater the Fe_2O_3/TiO_2 ratio, the better the drainage conditions. According to Bispo *et al*. (2011a), LVA and LA are better drained, with an Fe_2O_3/TiO_2 ratio that is 4–6 times greater than those of GXbd and LAC, which have similar values.

The chemical attributes together with XRD allowed the identification of the mineral constituents of the soil in this study. X-ray diffraction patterns of the silt sample of the LAC soil (Fig. 1), obtained after drying the sample at 105°C, display peaks that are attributed to anatase (TiO_2), a 2:1 phyllosilicate classified as illite (typically $K_{0.75}(Al_{.1.75}R^{2+}_{0.25})(Si_{3.50}Al_{0.5})O_{10}(OH)_2$; Bailey *et al*., 1984), kaolinite and/or dehydrated halloysite ($Al_2Si_2O_5(OH)_4$), quartz (SiO_2), and silicon ('Si') that was admixed as an internal standard. Neither magnetite nor hematite was detected. The XRD reflections at 0.715 nm (0 0 1) and 0.356 nm (0 0 2) allow the identification of kaolinite (Bish & Von Dreele, 1989). The reflections at 1.00 and 0.33 nm (Fig. 2) are consistent with the presence of a 2:1 phyllosilicate, e.g. illite, whereas drying the sample at 105°C should have irreversibly dehydrated 1.0 nm halloysite (Kohyama *et al*., 1978). A relatively intense reflection at 0.445 nm can be taken to indicate the presence of some dehydrated (0.7 nm) halloysite, the intensity of the (0 2 11) peak of which is more than half as great as that of the basal (0 0 1) peak at 0.715 nm (Brindley, 1961). The fitted lines presented in Figs 1 and 2 were obtained by Rietveld refinement using MAUD software (Lutterotti, 2010) with the following ICSD structures: ICSD 51688 (Si), ICSD 63192 (kaolinite), ICSD 9852 (anatase), ICSD 27745 (quartz), and ICSD 90144 (illite). For kaolinite and illite, the single-layer model for stacking faults (Ufer *et al*., 2004) had to be used to account for the disorder shown in the measured XRD. Kämpf & Curi (2003) suggested that the lower stability of halloysite (which is more common in soils of volcanic deposits and in early weathering stages) than that of kaolinite was responsible for the scarcity of this clay mineral in Brazilian soils, although minor amounts of dehydrated 0.7 nm halloysite associated with kaolinite have been identified in Brazilian Ultisols, Oxisols and Entisols.

Mössbauer spectra of the silt fraction of the LAC soil, taken at room temperature (298 K) and 80 K, are shown in Fig. 3 (parts a and b, respectively). The hyperfine parameters are given in Table 2. A first,

https://doi.org/10.1180/claymin.2015.050.4.02 Published online by Cambridge University Press

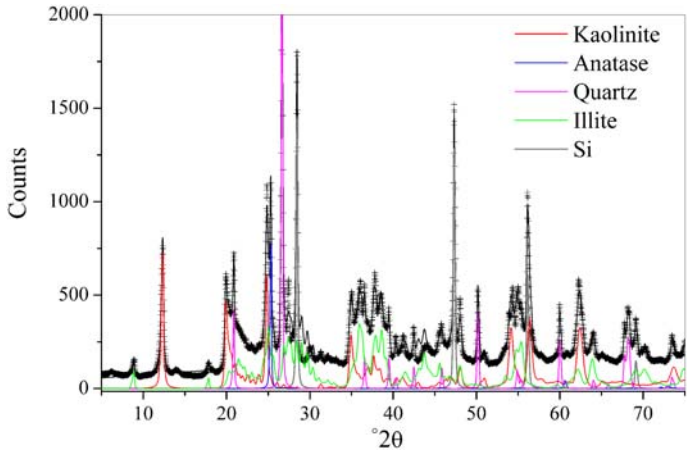

FIG. 1. Powder XRD pattern of the silt fraction of the Grey Latosol (LAC) in the range $4° \leq 2\theta \leq 80°$. The full line represents the Rietveld refinement obtained with the species shown separately at bottom.

statistically acceptable fit of the room-temperature spectrum indicated two doublets that could be attributed to Fe^{3+} and one to Fe^{2+}. The isomer shift of the Fe^{2+} doublet (1.80 mm/s), however, was unrealistically high. An alternative fit of a spectrum of this sample, taken in a narrower velocity range of ±4 mm/s, could be fitted with two Fe^{3+} and Fe^{2+} doublets, the latter having more realistic values (Fig. 3a and Table 2). This Mössbauer spectrum indicates ~25 atom.% of the iron to be present in the chemically reduced form as Fe^{2+}. The different Fe^{3+} isomer shifts, in agreement with tetrahedral and octahedral coordination, point furthermore to an iron oxide spinel, possibly maghemite (γ-Fe_2O_3), in the mineral fraction of this soil. At 80 K, the spectrum of the LAC silt can be fitted with three paramagnetic doublets, indicating one Fe^{3+} and two Fe^{2+} sites, plus one magnetic sextet with a zero quadrupole shift that probably results from maghemite (Silva *et al*., 2013) (Fig. 3b, Table 2). Mössbauer spectroscopy thus indicates that the sextet is due to maghemite, whereas the doublets at 80 K are attributed to octahedral Fe^{3+} in kaolinite and Fe^{2+},

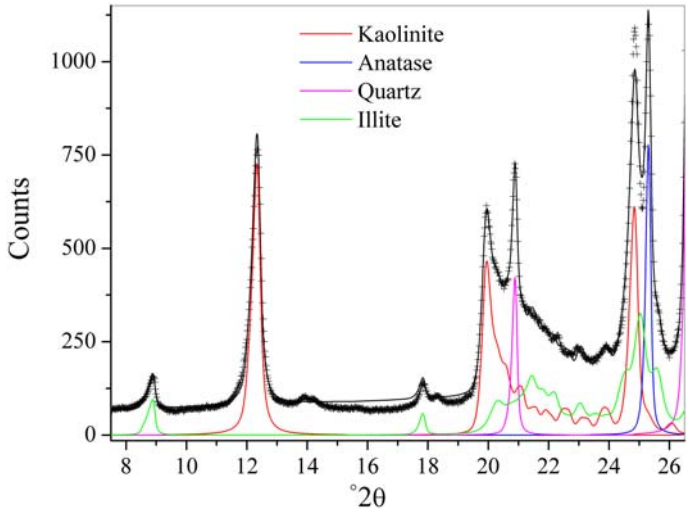

FIG. 2. Powder XRD pattern of the silt fraction of the Grey Latosol (LAC) in the range $7° \leq 2\theta \leq 26°$ (enlarged extract from Fig.1).

https://doi.org/10.1180/claymin.2015.050.4.02 Published online by Cambridge University Press

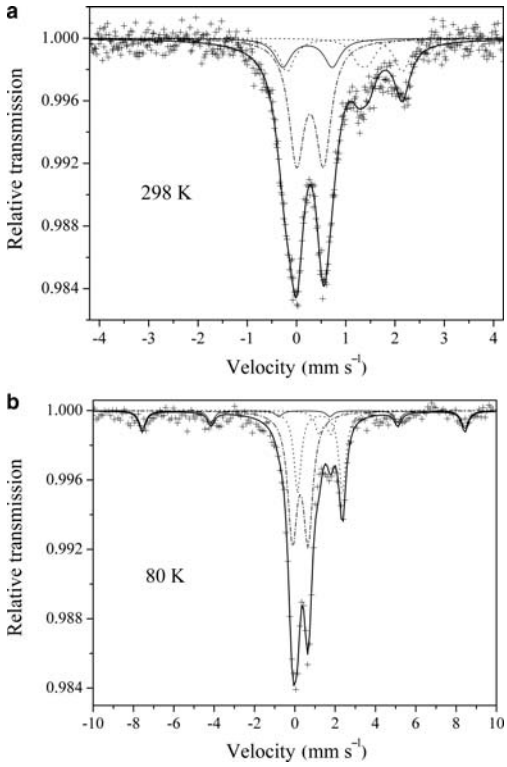

FIG. 3. Mössbauer spectra at 298 K (a) and 80 K (b) of the silt fraction of the Grey Latosol (LAC).

possibly together with some of the Fe^{3+}, in a 2:1 phyllosilicate such as illite (Murad & Wagner, 1994).

The ESR spectra show broad signals along the field scan up to 3600 Oe. To avoid the complications arising from a residual non-random particle orientation, the samples were ground manually. The resultant homogeneous samples give spectra such as that shown in Fig. 4.

ESR shows irregular features which can be attributed to a residual orientation of the grains. Disregarding these minor features, the spectrum could be fit with four resonance lines, the parameters of which are given in Table 3. The broader and intense zero-field (resonance line A) is attributed to the ferrimagnetic contribution from maghemite. The other three lines are due to paramagnetic Fe^{3+} in different sites.

Maghemite, the γ-form of Fe_2O_3 has a disordered ferric spinel (AB_2O_4) structure, in which the A cations have a regular tetrahedral coordination by oxygen and the B cations are octahedrally coordinated by oxygen (with a local trigonal distortion, although the crystal symmetry is cubic). Maghemite can be considered an Fe^{2+}-deficient magnetite. There are insufficient Fe^{3+}

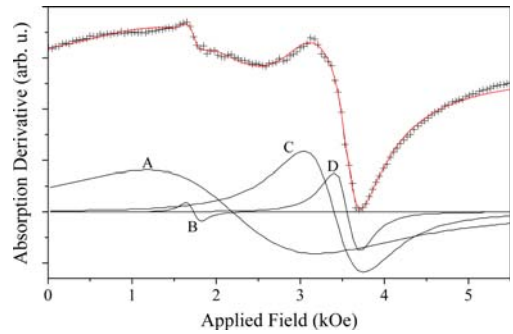

FIG. 4. ESR spectrum of a representative sample (crosses) of the silt fraction of the 'Grey Latosol'. The envelope is the fitted curve resulting from the sum of the lines labelled A–D, which are described in Table 3.

cations to fill all the A and B sites. The resonance line B with an effective g value $g_{ef} = 4.10$ corresponds to a rather distorted octahedral Fe^{3+} site which imparts strong crystal fields (Castner *et al*., 1960; Manhães *et al*., 2003; Gopal *et al*., 2004), whereas lines C and D correspond to Fe^{3+} sites in a weak crystal field and symmetric octahedral sites. As Fe^{3+} has zero orbital angular momentum in the free atom, lines close to the free-spin value $g = 2$ are expected. From the line intensities it is clear that the number of distorted sites is much smaller than the weakly and/or non-distorted sites. Line D is also assigned in the present sample to Fe^{3+}, although there are reports of the occurrence of two signals around $g_{ef} = 2$ in kaolinite (Komusiński *et al*., 1981). The ESR is not able to detect Fe^{2+} at the frequency and temperature available in the equipment used (Orton, 1959; Mota *et al*., 2009).

Studies exist associating ESR lines with $g_{ef} \approx 2$ to Ti^{3+} in a titania matrix (e.g. Iacomi *et al*., 2007). Ti^{3+} can occur in the structure of anatase as a result of

TABLE 3. ESR parameters of the silt fraction of the Grey Latosol (LAC) from Fig. 4. The uncertainties of g_{ef} are of the order of 0.05. H_{res} for resonance field and ΔH for linewidth.

	Resonance lines			
	A	B	C	D
	Ferrimagnetic	-------Paramagnetic-------		
g_{ef}	–	4.10	2.07	1.98
H_{res} (kOe)	2189	1735	3400	3556
ΔH (kOe)	1.740	0.139	0.617	0.264

https://doi.org/10.1180/claymin.2015.050.4.02 Published online by Cambridge University Press

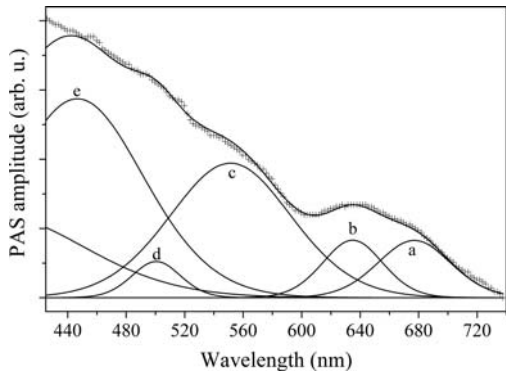

FIG. 5. Amplitude of the photoacoustic signal of the silt fraction of the Grey Latosol as a function of the wavelength of the incident light (crosses). The envelope results from the sum of the absorption bands labelled a–e, which are described in Table 4.

charge unbalance and vacancies. The hypothesis that there is a contribution by Ti^{3+} to the D line detected by EPR cannot be ignored, therefore. Another aspect which might influence the physicochemical properties is the fact that Fe and Ti with different valences can easily substitute for each other. In this way, the presence of both Fe^{3+} and Fe^{2+} in the titanium oxides, as well as the occurrence of mixed Fe-Ti oxides is possible, and may affect the ESR and Mössbauer results (e.g. Scorzelli *et al*., 2008).

A typical PAS result with six fitted absorption bands is presented in Fig. 5. The peak positions and the corresponding assigned interpretations are given in Table 4.

No isolated peak or band is observed in the optical region so the distribution of broad bands over the whole spectral range is related to the greyish appearance of the soil. The predominant monotonic decay of the absorption curve should not favour a particular colour, although there is some prominence of Fe absorption above 630 nm. This rising slope of the optical absorption is common in kaolinite samples and can be related to light scattering by small particles (Karickhoff & Bailey, 1973; Hunt, 1977; Malengreau *et al*., 1994). Note that the amount of Ti can be related to the large tail of a band with maximum close to 400 nm ($^6A_1 \rightarrow {}^4T_2$ (^4D)) (Gunasekaran & Anbalagan, 2008), but this is difficult to confirm as the signal is as broadly distributed as a background. Manganese and Ti ions may contribute to the absorption, but the spectrum is dominated by iron absorption bands. The bands at 680 nm and 510 nm correspond to Fe^{3+} in octahedral sites of kaolinite or halloysite structures (Malengreau *et al*., 1994). Considering the electron energy level diagram, these sites are probably responsible for the ESR signals B and C (Gunasekaran & Anbalagan, 2008; Gopal *et al*., 2004). There are possible transitions in the Tanabe and Sugano diagrams which could match these values both with weak and strong crystal fields. The absorptions at ~550 nm and 450 nm have been reported in reference samples of maghemite and hematite (Malengreau *et al*., 1994). The detection of maghemite by Mössbauer spectroscopy indicates that these absorptions might result from tetrahedrally and octahedrally coordinated Fe^{3+} of maghemite particles and thus relates to the ESR lines labelled A and D. The line A originates from magnetically ordered maghemite, whereas the paramagnetic signal D might result from maghemite particles that are too small to be ordered. In this case, paramagnetic Fe^{3+} would be in a weak crystal field compatible with the transition $^6A_1 \rightarrow {}^4E_g$, $^6A_1$(G) (Gunasekaran and Anbalagan, 2008). Ageing of ferrihydrite precipitated in the presence of ligands capable of ligand exchange with Fe–OH surface groups has been suggested as a possible formation mechanism for pedogenic maghemite of small (10 to

TABLE 4. Optical transitions observed by PAS analysis of the silt fraction of the Grey Latosol (LAC) from Fig. 5.

Peak position	Label	Oxidation state	Transition
680 nm	a	Fe^{3+}	$^6A_1 \rightarrow {}^4T_1$ (G)
650 nm	b	Fe^{2+}	$^5T_2 \rightarrow {}^3T_2$ (H)
550 nm	c	Fe^{3+}	$^6A_1 \rightarrow {}^4T_1$ (G) or $^6A_1 \rightarrow {}^4T_2$ (D)
510 nm	d	Fe^{3+}	$^6A_1 \rightarrow {}^4T_2$ (G)
450 nm	e	Fe^{3+}	$^6A_1 \rightarrow {}^4T_2$ (G) or $^6A_1 \rightarrow {}^4E_g$, $^6A_1$(G)

https://doi.org/10.1180/claymin.2015.050.4.02 Published online by Cambridge University Press

30 nm) particle size with minimal *ad hoc* assumptions (Barrón & Torrent, 2002). This may be the case here.

The absorption at 650 nm is more difficult to interpret. Bands in this wavelength are not expected in kaolinite and halloysite (Hunt, 1977; Malengreau *et al*., 1994). However, such a band can also be assigned to Fe^{2+} in an octahedrally coordinated site in minerals (Gunasekaran & Anbalagan, 2008). This is also supported by energy-level diagrams with a weak octahedral crystal field, so that PAS confirms the presence of Fe^{2+} shown by Mössbauer spectroscopy.

Motivation for a new soil suborder

Deeply weathered soils, identified as Latossolos in the Brazilian system, corresponding to Oxisols, Sols Ferralitiques or Ferralsols of the American, French and FAO soil classification systems, respectively, are the most common soils in Brazil, covering >60% of the country by area (Schaefer *et al*., 2008). Goethite (α-FeOOH), indicated by yellowish colours (2.5Y–10YR in the absence of hematite), and hematite (α-Fe_2O_3), which imparts reddish colours (2.5YR–5R), even when present in very minor amounts, are among the most abundant pedogenic oxides in these soils and therefore determine the soil colours. The FAO soil classification (IUSS Working Group WRB, 2014), for example, thus states that "Ferralsols represent the classical, deeply weathered, red or yellow soils of the humid tropics", whereas in Soil Taxonomy it is stated that "The unique properties of Oxisols are extreme weathering of most minerals other than quartz to kaolin and free oxides" (Soil Survey Staff, 1999).

Both goethite and hematite are missing from the greyish Oxisols described here, and the colour originates essentially from the presence of iron-bearing kaolinite. Such Greyish Latossols, resulting from leaching and precipitation are widespread in tropical regions, and have been described from numerous localities throughout Brazil (e.g. Resende *et al*., 1980; Teófilo & Frota, 1982; Dubroeucq & Volkoff, 1998; Ker *et al*., 2005; Ferreira *et al*., 2010; Bispo *et al*., 2011a,b), in India (Peterschmitt *et al*., 1996), Indonesia (Tan, 2008) and elsewhere in tropical regions (Alvim & Kozlowski, 1977). This is in agreement with carbon isotope data that indicate temporal variations, changing the setting in the Late Pleistocene and Holocene from a waterlogged, reducing environment characterized by a grey soil colour and lack of free Fe oxides to the current dry situation, retaining the mineralogy and colour (Munsell 10YR) in the process (Bispo & Silva, 2014). The present study presents the basic data for a new suborder to be considered for Latossols in the Brazilian soil classification, for which we propose the name "Latossolo Acinzentado", literally 'Greyish Lattosol' in Portuguese, i.e. greyish Oxisol or Ferralsol. This is repeatedly abbreviated as LAC in the present paper, which should not be confused with the term LAC for low-activity clay in Soil Taxonomy (Soil Survey Staff, 1999).

CONCLUSIONS

A physicochemical characterization of the silt fraction of a Grey Latosol from a '*vereda*' of the Jequitinhonha Valley in Brazil has been carried out using several techniques. Mössbauer and ESR results show the presence of Fe^{2+} and Fe^{3+} in different structural sites. The measured parameters point to Fe^{3+} in distorted octahedral sites as well as in symmetric or weakly distorted sites. Mössbauer and ESR spectra are relatively broad, demonstrating a large distribution of local environment around the Fe ions, i.e. a large distribution of site distortions. As a consequence of this physical aspect, the soil is able to absorb and reflect almost continuously through the whole visible-light spectrum, leading to its greyish appearance. The light absorption spectrum has been measured indirectly using PAS and fitted considering typical optical transitions of Fe^{2+} and Fe^{3+}, which are the dominant colour centres. Kaolinite (and conceivably dehydrated halloysite, the presence of which cannot be excluded) as well as anatase have been identified by XRD. Through substitution, Fe ions can be present in all of these minerals. Because of the mineralogical complexity of the soil, XRD, Mössbauer and ESR present superimposed signals that complicate a clear and unambiguous determination of the precise location of the Fe ions. Nevertheless, because of the predominance of the phyllosilicates and their structures, it seems likely that most of the iron is in the structure of kaolinite (and possibly dehydrated halloysite). A minor amount of maghemite was also detected.

ACKNOWLEDGMENTS

The authors are indebted to Janice Bishop and Balwant Singh for helpful reviews which led to significant improvement of the manuscript. Financial support by FAPEMIG (Brazil) visitor research grant (# CAG-BPV-00065-14) to E. Murad and post-doctoral fellowship (grant # CAG-BPD-00032-11) to S. de Souza at UFVJM, from FAPERJ to A.O. Guimarães and H. Vargas, and

CAPES (Brazil) for granting the Visiting PVNS professorship to J.D. Fabris at UFVJM is also appreciated.

REFERENCES

Ab´Sáber A.N. (2000) The natural organization of Brazilian inter- and subtropical landscapes. *Revista do Instituto Geológico*, **21**, 57–70.

Alleoni L.R.F. & Camargo O.A. (1994) Pontos de efeito salino nulo de Latossolos Ácricos. *Revista Brasileira de Ciência do Solo*, **18**, 175–180.

Alvim P.T. & Kozlowski T.T. (1977) *Ecophysiology of Tropical Crops.* Academic Press Inc., London, 490 pp.

Bailey S.W., Brindley G.W., Fanning D.S., Kodama H. & Martin R. (1984) Report of The Clay Minerals Society Nomenclature Committee for 1982 and 1983. *Clays and Clay Minerals*, **32**, 239–240.

Barrón V. & Torrent J. (2002) Evidence for a simple pathway to maghemite in Earth and Mars soils. *Geochimica et Cosmochimica Acta*, **66**, 2801–2806.

Bish D.L. & Von Dreele R.B. (1989) Rietveld refinement of non-hydrogen atomic positions in kaolinite. *Clays and Clay Minerals*, **37**, 289–296.

Bispo F.A.B. & Silva A.C. (2014) Solos de vereda do alto Vale do Jequitinhonha – Minas Gerais – Brasil: testemunho de mudanças paleoambientais. *Extended Abstract, 20th Latin-American Congress and 16th Peruvian Congress of Soil Science*. Cusco, Peru.

Bispo F.H.A., Silva A.C. & Torrado P.V. (2011a) Highlands of the upper Jequitinhonha valley, Brazil. I – characterization and classification. *Revista Brasileira de Ciência do Solo*, **35**, 1069–1080.

Bispo F.H.A., Silva A.C., Vidal Torrado P. & Souza Junior V.S. (2011b) Highlands of the upper Jequitinhonha valley, Brazil: II – Mineralogy, micromorphology, and landscape evolution. *Revista Brasileira de Ciência do Solo*, **35**, 1081–1091.

Breemen N. van & Buurman P. (2002) *Soil Formation, 2nd edition.* Kluwer Academic, Dordrecht, The Netherlands, 404 pp.

Brindley G.W. (1961) Kaolin, serpentine and kindred minerals. Pp. 51–131 in: *The X-ray Identification and Crystal Structures of Clay Minerals* (G. Brown, editor). The Mineralogical Society, London.

Castner T. Jr., Newell G.S., Holton W.C. & Slichter C.P. (1960) Note on the paramagnetic resonance of iron in glass. *Journal of Chemical Physics*, **32**, 668–673.

Cheburkin A.K. & Shotyk W. (1996) An energy-dispersive miniprobe multielement analyzer (EMMA) for direct analysis of Pb and other trace elements in peats. *Fresenius' Journal of Analytical Chemistry*, **354**, 688–691.

Coelho M.R., Vidal-Torrado P. & Ladeira F.S.B. (2001) Macro e micromorfologia de ferricretes nodulares desenvolvidos de Arenito do Grupo Bauru, Formação Adamantina. *Revista Brasileira de Ciência do Solo*, **25**, 371–385.

Costa-Milanez C.B., Lourenço-Silva G., Castro P.T.A., Majer J.D. & Ribeiro S.P. (2014) Are ant assemblages of Brazilian veredas characterised by location or habitat type? *Brazilian Journal of Biology*, **74**, 89–99.

Dubroeucq D. & Volkoff B. (1998) From Oxisols to Spodosols and Histosols: evolution of the soil mantles in the Rio Negro basin (Amazonia). *Catena*, **32**, 245–280.

Deer W.A., Howie RA. & Zussman J. (2013) *An Introduction to the Rock-Forming Minerals*, 3rd edition. The Mineralogical Society, London.

EMBRAPA – Empresa Brasileira de Pesquisa Agropecuária (1997) Centro Nacional de Pesquisa de Solos. *Manual de Métodos de Análise de Solos*, 2nd ed., Embrapa Solos, Rio de Janeiro, Brazil, 212 pp.

Ferreira C.A., Silva A.C., Vidal-Torrado P.V. & Rocha W.W. (2010) Genesis and classification of Oxisols in a highland toposequence of the upper Jequitinhonha valley (MG). *Revista Brasileira de Ciência do Solo*, **34**, 195–209.

Gopal N.O., Narasimhulu K.V. & Lakshmana Rao J. (2004) Optical absorption, EPR, infrared and Raman spectral studies of clinochlore mineral. *Journal of Physics and Chemistry of Solids*, **65**, 1887–1893.

Gunasekaran S. & Anbalagan G. (2008) Optical absorption and EPR studies on some natural carbonate minerals. *Spectrochimica Acta A*, **69**, 383–390.

Hunt G.R. (1977) Spectral signatures of particulate minerals in the visible and near infrared. *Geophysics*, **42**, 501–513.

Iacomi F., Mardare D., Grecu M.N., Macovei D. & Ioan Vida-Simiti D. (2007) The influence of the substrate nature on the iron repartition in the titania matrix. *Surface Science*, **601**, 2692–2695.

IUSS Working Group WRB (2014) World Reference Base for Soil Resources 2014. International soil classification system for naming soils and creating legends for soil maps. *World Soil Resources Reports No. 106*. FAO, Rome.

Kämpf N. & Curi N. (2003) Argilominerais em solos brasileiros. Tópicos em ciência do solo. Viçosa, MG. *Sociedade Brasileira de Ciência do Solo*, **3**, 1–54

Karickhoff S.W. & Bailey G.W. (1973) Optical absorption spectra of clay minerals. *Clays and Clay Minerals*, **21**, 59–70.

Ker J.C. (1998) Latossolos do Brasil: Uma revisão. *Geonomos*, **5**, 17–40.

Ker J.C. , Carvalho Filho A., Oliveira V.C. & Santos H.G., editors. (2005) Reunião Nacional de Correlação de Solos – MG (VII RCC). *Guia de excursão. Sociedade Brasileira de Ciência do Solo*. Universidade Federal de Viçosa, Viçosa – MG, 39–44.

Kohyama N., Fukushima K. & Fukami A. (1978) Observation of the hydrated form of tubular halloysite

https://doi.org/10.1180/claymin.2015.050.4.02 Published online by Cambridge University Press

by an electron microscope equipped with an environmental cell. *Clays and Clay Minerals*, **26**, 25–40.

Komusiński J., Stoch L. & Dubiel S.M. (1981) Application of electron paramagnetic resonance and Mössbauer spectroscopy in the investigation of kaolinite-group minerals. *Clays and Clay Minerals*, **29**, 23–30.

Lutterotti L. (2010) Total pattern fitting for the combined size–strain–stress–texture determination in thin film diffraction. *Nuclear Instruments and Methods in Physics Research Section B: Beam Interactions with Materials and Atoms*, **268**, 334–340.

Malengreau N., Muller J.P. & Calas G. (1994) Fe-speciation in kaolins: a diffuse reflectance study. *Clays and Clay Minerals*, **42**, 137–147.

Manhães R.S.T. Auler L.T., Sthel M.S., Alexandre J., Massunaga M.S.O., Carrió J.G., dos Santos D.R., da Silva E.C., Garcia-Quiroz A. & Vargas H. (2003) Soil characterisation using X-ray diffraction, photoacoustic spectroscopy and electron paramagnetic resonance. *Applied Clay Science*, **21**, 303–311.

McKeague J.A. & Day J.H. (1966) Dithionite and oxalate extractable Fe and Al as aids in differentiating various classes of soils. *Canadian Journal of Soil Science*, **46**, 13–22.

Mehra O.P. & Jackson M.L. (1960) Iron oxide removal from soils and clay by a dithionite-citrate system buffered with sodium bicarbonate. *Clays and Clay Minerals*, **7**, 317–327.

Mestdagh M.M., Vielvoye L. & Herbillon A.J. (1980) Iron in kaolinite: II. The relationship between kaolinite crystallinity and iron content. *Clay Minerals*, **15**, 1–13.

Mota L., Toledo R., Faria R.T. Jr., da Silva E.C., Vargas H. & Delgadillo-Holtfort I. (2009) Thermally treated soil clays as ceramic raw materials: characterization by X-ray diffraction, photoacoustic spectroscopy and electron spin resonance. *Applied Clay Science*, **43**, 243–247.

Murad E. & Cashion J. (2004) *Mössbauer Spectroscopy of Environmental Materials and their Industrial Utilization.* Kluwer Academic Publishers, Boston, Massachusetts, USA, 418 pp.

Murad E. & Wagner U. (1991) Mössbauer spectra of kaolinite, halloysite and the firing products of kaolinite: new results and a reappraisal of published work. *Neues Jahrbuch für Mineralogie, Abhandlungen*, **162**, 281–309.

Murad E. & Wagner U. (1994) The Mössbauer spectrum of illite. *Clay Minerals*, **29**, 1–10.

Oliveira J.B., Resende M. & Curi N. (1991) Caracterização e classificação de Latossolos variação una e de solos afins da região de Guaíra, SP. *Revista Brasileira de Ciência do Solo*, **15**, 207–218.

Orton J.W. (1959) Paramagnetic resonance data. *Reports on Progress in Physics*, **22**, 204–240.

Pedrosa-Soares A.C., Noce C.M., Vida P., Monteiro R.L. B.P. & Leonardos O.H. (1992) Towards a new tectonic model for the Late Proterozoic Araçuaí (SE Brazil) – West Congolian (SW Africa) belt. *Journal of South American Earth Sciences*, **6**, 33–47.

Peterschmitt E., Fritsch E., Rajot J.L. & Herbillon A.J. (1996) Yellowing, bleaching and ferritisation processes in soil mantle of the Western Ghâts, South India. *Geoderma*, **74**, 235–253.

Resende M., Carmo D.N., Silva T.C.A., Batista R.B. & Rocha D. (1980) *Levantamento de reconhecimento, com detalhes, de solos de chapadas do alto Jequitinhonha.* Universidade Federal de Viçosa, Viçosa, MG, 133 pp.

Schaefer C.E.G.R., Fabris J.D. & Ker J.C. (2008) Minerals in the clay fraction of Brazilian Latosols (Oxisols): a review. *Clay Minerals*, **43**, 137–154.

Schwertmann U. (1964) Differenzierung der Eisenoxide des Bodens durch Extraktion mit Ammoniumoxalat-Lösung. *Zeitschrift für Pflanzenernährung und Bodenkunde*, **105**, 194–202.

Scorzelli R.B., Bertolino L.C., Luz A.B., Duttine M., Silva F.A.N.G. & Munyaco P. (2008) Spectroscopic studies of kaolin from different Brazilian regions. *Clay Minerals*, **43**, 129–135.

Silva A.C., Rocha W.W., Ferreira C.A., Campos J.R., Bispo F.H., A., Romão, R.V. & Nunciato, G.V. (2010) *Levantamento pedológico, determinação da aptidão agrícola e avaliação do risco de erosão das terras da ArcelorMittal Jequitinhonha no Vale do Jequitinhonha – MG.* Capelinha – MG, ArcelorMittal Jequitinhonha, 133 pp.

Silva A.C., Bispo F.H.A., de Souza S., Ardisson J.D., Viana A.J.S., Pereira M.C., Costa F.R., Murad E. & Fabris J.D. (2013) Iron mineralogy of a grey Oxisol from the Jequitinhonha River Basin, Minas Gerais, Brazil. *Clay Minerals*, **48**, 713–723.

Soil Survey Staff (1999) *Soil Taxonomy: a basic system of soil classification for making and interpreting soil surveys*. United States Department of Agriculture – Natural Resources Conservation Service, Agriculture Handbook No. 436. U.S. Government Printing Office, Washington, DC. ftp://ftp-fc.sc.egov.usda.gov/NSSC/Soil_Taxonomy/tax.pdf (accessed 23.01.2015).

Stucki J.W. &. Kostka J.E. (2006) Microbial reduction of iron in smectite. *Comptes Rendus Geoscience*, **338**, 468–575.

Tan K.H. (2008) *Soils in the Humid Tropics and Monsoon Region of Indonesia.* CRC Press, Taylor & Francis Group, Boca Raton, Florida, USA, 556 pp.

Teófilo F.H.P. & Frota J.N.E. (1982) Formas de fósforo e sua disponibilidade em solos da região da Ibiapaba-CE. *Ciência Agronomica*, **13**, 61–69.

Ufer K., Roth G., Kleeberg R., Stanjek H., Dohrmann R. & Bergmann J. (2004) Description of X-ray powder pattern of turbostratically disordered layer structures with a Rietveld compatible approach. *Zeitschrift für Kristallographie*, **219**, 519–527.

https://doi.org/10.1180/claymin.2015.050.4.02 Published online by Cambridge University Press